

Mathematical Modeling for Thermoelastic Double Porous Micro-Beam Resonators

R. Kumar¹, R. Vohra^{2,*}, M.G. Gorla²

¹*Department of Mathematics, Kurukshetra University, Kurukshetra, Haryana, India*

²*Department of Mathematics & Statistics, H.P. University, Shimla, HP, India*

Received 8 February 2018; accepted 29 March 2018

ABSTRACT

In the present work, the mathematical model of a homogeneous, isotropic thermoelastic double porous micro-beam, based on the Euler-Bernoulli theory is developed in the context of Lord-Shulman [1] theory of thermoelasticity. Laplace transform technique has been used to obtain the expressions for lateral deflection, axial stress, axial displacement, volume fraction field and temperature distribution. A numerical inversion technique has been applied to recover the resulting quantities in the physical domain. Variations of axial displacement, axial stress, lateral deflection, volume fraction field and temperature distribution with axial distance are depicted graphically to show the effects of porosity and thermal relaxation time. Some particular cases are also deduced.

© 2018 IAU, Arak Branch. All rights reserved.

Keywords: Double porosity; Thermoelasticity; Lord-shulman theory; Micro-beam.

1 INTRODUCTION

PORES and fractures can be seen in engineering structures due to reasons like erosion, corrosion, fatigue or accidents which affect the dynamic behavior of the entire structure to a considerable extent. This leads to the development of double porosity model which has its applications in geophysics, rock mechanics and many branches of engineering like civil engineering, chemical engineering and the petroleum industry. Biot [2] proposed model for porous media with single porosity. Later on Barenblatt et al. [3] introduced a model for porous media with double porosity structure. The double porosity model consists of two coexisting degrees of porosity in which one corresponds to porous matrix and other corresponds to fissure matrix. Aifantis [4-6] introduced a multi-porous system and studied the mechanics of diffusion in solids. Wilson and Aifantis [7] presented the theory of consolidation with the double porosity. Khaled et. al [8] employed a finite element method to consider the numerical solutions of the differential equation of the theory of consolidation with double porosity developed by Wilson and Aifantis [7]. Beskos and Aifantis [9] presented the theory of consolidation with double porosity-II and obtained the analytical solutions to two boundary value problems. Khalili and Selvadurai [10] presented a fully coupled constitutive model for thermo-hydro –mechanical analysis in elastic media with double porosity structure. Various authors [11-13] investigated problems for elastic solids and thermoelastic solids in the theory of thermoelasticity with double porosity based on Darcy's law. Nunziato and Cowin [14] developed a nonlinear theory of elastic material with voids. Later, Cowin and Nunziato [15] developed a theory of linear elastic materials with

*Corresponding author. Tel.: +91 9418188775.
E-mail address: richavhr88@gmail.com (R.Vohra).

voids for the mathematical study of the mechanical behavior of porous solids. Iesan and Quintanilla [16] derived a theory of thermoelastic solids with double porosity structure by using the theory developed by Nunziato and Cowin. Darcy's law is not used in developing this theory. So far not much work has been done on the theory of thermoelasticity with double porosity based on the model proposed by Iesan and Quintanilla [16]. Recently investigations have been started in the theory of thermoelasticity with double porosity [16] which has a significant application in continuum mechanics. The demand for engineering structures is continuously increasing. Aerospace vehicles, bridges, and automobiles are examples of these structures. Many aspects have to be taken into consideration in the design of these structures to improve their performance and extend their life. One aspect of the design process is the dynamic response of structures. The dynamics of distributed parameter and continuous systems, like beams, were governed by linear and nonlinear partial differential equations in space and time. Micro-scale mechanical resonators have high sensitivity as well as fast response and are widely used as sensors and modulators. Recently, micro- and nano-mechanical resonators have attracted considerable attention due to their many important technological applications. Accurate analysis of various effects on the characteristics of resonators, such as resonant frequencies and quality factors, is crucial for designing high-performance components. Micro beam resonators are gaining popularity in modern technologies, such as atomic force microscope, sensing sequence-specific DNA, mass sensors, resonators, chemical sensors and pressure sensors [17-20]. Scientists have continuously investigated the potential of these devices to apply them for different applications. Nowadays, their existence became indispensable in many fields and the continuous development hopefully lead to more importance in future. One of the useful ways to study the micro beam resonators is the vibration response analysis. Vibration analysis can be used directly to quantify system performance and designing such devices. The vibration problems of uniform Euler- Bernoulli beams can be solved by analytical or approximate approaches [21, 22]. Boley [23] analyzed the vibrations of a simply supported rectangular beam subjected to a suddenly applied heat input distributed along its span. Manolis and Beskos [24] examined the thermally induced vibration of structures consisting of beams exposed to rapid surface heating. Huniti et al. [25] investigated the thermally induced displacements and stresses of a rod using the Laplace transformation technique. Biondi and Caddemi [26] studied the problem of the integration of the static governing equations of the uniform Euler-Bernoulli beams with discontinuities, considering the flexural stiffness and slope discontinuities. Fang et al. [27] analyzed the vibrations in micro beam resonators induced by laser. Sharma and Grover [28] analysed the thermoelastic vibrations in micro-/nano-scale beam resonators with the presence of voids. Esen [29] investigated the analysis of transverse and longitudinal vibrations of a thin plate which carries a load moving along an arbitrary trajectory with variable velocity. Kumar [30] studied the response of thermoelastic beam due to thermal source in modified couple stress theory. Various authors [31-36] investigated vibration analysis of micro beam in different theories of thermoelasticity.

In the present paper, the mathematical model of a homogeneous, isotropic thermoelastic double porous micro beam, based on the Euler-Bernoulli theory is developed in the context of Lord-Shulman [1] theory of thermoelasticity. Laplace transform has been applied to find the expressions for lateral deflection, axial stress, axial displacement, volume fraction fields and temperature distribution. The resulting quantities are obtained in the physical domain by using a numerical inversion technique. Variations of axial displacement, axial stress, lateral deflection, and volume fraction field and temperature distribution with axial distance are depicted graphically to show the effects of porosity and thermal relaxation time. Some particular cases have also been deduced.

2 BASIC EQUATIONS

Following Iesan and Quintanilla [16] and Lord and Shulman [1]; the constitutive relations and field equations for homogeneous isotropic thermoelastic material with double porosity structure in the absence of body forces, extrinsic equilibrated body forces and heat sources can be written as:

Equations of motion

$$\mu \nabla^2 u_i + (\lambda + \mu) u_{j,ji} + b \varphi_{,i} + d \psi_{,i} - \beta T_{,i} = \rho \ddot{u}_i, \quad (1)$$

Equilibrated stress equations of motion

$$\alpha \nabla^2 \varphi + b_1 \nabla^2 \psi - b u_{r,r} - \alpha_1 \varphi - \alpha_3 \psi + \gamma_1 T = \kappa_1 \ddot{\varphi}, \quad (2)$$

$$b_1 \nabla^2 \varphi + \gamma \nabla^2 \psi - du_{r,r} - \alpha_3 \varphi - \alpha_2 \psi + \gamma_2 T = \kappa_2 \ddot{\psi}, \quad (3)$$

Equation of heat conduction

$$\left(1 + \tau_0 \frac{\partial}{\partial t}\right) (\beta T_0 \dot{u}_{j,j} + \gamma_1 T_0 \dot{\varphi} + \gamma_2 T_0 \dot{\psi} + \rho C^* \dot{T}) = K^* \nabla^2 T \quad (4)$$

Constitutive relation

$$t_{ij} = \lambda e_{rr} \delta_{ij} + 2\mu e_{ij} + b\varphi \delta_{ij} + d\psi \delta_{ij} - \beta T \delta_{ij} \quad (5)$$

where λ and μ are Lamé's constants, ρ is the mass density; $\beta = (3\lambda + 2\mu)\alpha_t$; α_t is the linear thermal expansion; C^* is the specific heat at constant strain, u_i is the displacement components; t_{ij} is the stress tensor; κ_1 and κ_2 are coefficients of equilibrated inertia; φ is the volume fraction field corresponding to pores and ψ is the volume fraction field corresponding to fissures; K^* is the coefficient of thermal conductivity; τ_0 is the thermal relaxation time, κ_1 and κ_2 are coefficients of equilibrated inertia and $b, d, b_1, \gamma, \gamma_1, \gamma_2$ are constitutive coefficients; δ_{ij} is the Kronecker's delta; T is the temperature change measured from the absolute temperature T_0 ($T_0 \neq 0$); a superposed dot represents differentiation with respect to time variable t .

3 FORMULATION OF THE PROBLEM

Let us consider a thermoelastic double porous micro beam along the axial direction (x -axis) of the beam. The beam has cross-sectional area A , moment of inertia I , length L , width a and thickness h as shown in the Fig.1.

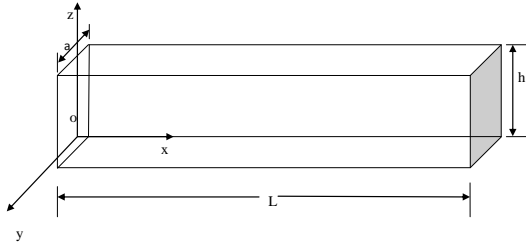


Fig.1
Geometry of the beam.

The micro beam undergoes bending vibrations of small amplitude about the x -axis such that the deflection is consistent with the linear Euler-Bernoulli theory. Therefore, the displacements can be written as:

$$u_1 = u = -z \frac{\partial w}{\partial x}, \quad u_2 = 0, \quad u_3 = w(x, t) \quad (6)$$

where w is the lateral deflection and u is the axial displacement. The equation of motion of free flexural vibrations of the beam is given by

$$\frac{\partial^2 M}{\partial x^2} + \rho A \left(\frac{\partial^2 w}{\partial t^2} \right) = 0 \quad (7)$$

where $A = ah$ is the cross-section area and M the flexural moment of cross section of micro beam. The flexural moment of the cross section of the beam is given by

$$M(x,t) = -a \int_{-h/2}^{h/2} t_x z dz = (\lambda + 2\mu)I \frac{\partial^2 w}{\partial x^2} - M_\varphi - M_\psi + M_T \tag{8}$$

where $I = ah^3/12$ is the moment of inertia of the cross-section and M_φ, M_ψ are the volume fraction field moments and M_T is thermal moment of the beam and are given by

$$M_\varphi = b \int_{-h/2}^{h/2} a\varphi z dz, \quad M_\psi = d \int_{-h/2}^{h/2} a\psi z dz, \quad M_T = \beta \int_{-h/2}^{h/2} aTz dz \tag{9}$$

Substituting Eq. (8) in Eq. (7), we get the equation of motion of the micro beam as:

$$(\lambda + 2\mu)I \frac{\partial^4 w}{\partial x^4} + \rho A \left(\frac{\partial^2 w}{\partial t^2} \right) - \frac{\partial^2 M_\varphi}{\partial x^2} - \frac{\partial^2 M_\psi}{\partial x^2} + \frac{\partial^2 M_T}{\partial x^2} = 0 \tag{10}$$

Eqs. (2)- (4) with the aid of Eq.(6) can be written as:

$$\alpha \left(\frac{\partial^2 \varphi}{\partial x^2} + \frac{\partial^2 \varphi}{\partial z^2} \right) + b_1 \left(\frac{\partial^2 \psi}{\partial x^2} + \frac{\partial^2 \psi}{\partial z^2} \right) + bz \frac{\partial^2 w}{\partial x^2} - \alpha_1 \varphi - \alpha_3 \psi + \gamma_1 T = \kappa_1 \frac{\partial^2 \varphi}{\partial t^2} \tag{11}$$

$$b_1 \left(\frac{\partial^2 \varphi}{\partial x^2} + \frac{\partial^2 \varphi}{\partial z^2} \right) + \gamma \left(\frac{\partial^2 \psi}{\partial x^2} + \frac{\partial^2 \psi}{\partial z^2} \right) + dz \frac{\partial^2 w}{\partial x^2} - \alpha_3 \varphi - \alpha_2 \psi + \gamma_2 T = \kappa_2 \frac{\partial^2 \psi}{\partial t^2} \tag{12}$$

$$K^* \left(\frac{\partial^2 T}{\partial x^2} + \frac{\partial^2 T}{\partial z^2} \right) = \left(1 + \tau_0 \frac{\partial}{\partial t} \right) \left[-\beta T_0 z \frac{\partial}{\partial t} \left(\frac{\partial^2 w}{\partial x^2} \right) + \gamma_1 T_0 \dot{\varphi} + \gamma_2 T_0 \dot{\psi} + \rho C^* \dot{T} \right] \tag{13}$$

4 SOLUTION OF THE PROBLEM

For the present micro beam, we assume that there is no flow of heat and volume fraction fields across the surfaces ($z = \pm h/2$) so that $\partial T / \partial z = \partial \varphi / \partial z = \partial \psi / \partial z = 0$ at $z = \pm h/2$. For a very thin beam, assuming that volume fraction fields and temperature increment in terms of $\sin(\pi z / h)$ function along the thickness direction. Therefore,

$$\varphi(x,z,t) = \Phi(x,t) \sin(\pi z / h), \quad \psi(x,z,t) = \Psi(x,t) \sin(\pi z / h), \quad T(x,z,t) = \Theta(x,t) \sin(\pi z / h) \tag{14}$$

Making use of Eq. (14) in Eq. (10) yields

$$(\lambda + 2\mu)I \frac{\partial^4 w}{\partial x^4} + \rho ah \left(\frac{\partial^2 w}{\partial t^2} \right) - \frac{2abh^2}{\pi^2} \frac{\partial^2 \Phi}{\partial x^2} - \frac{2adh^2}{\pi^2} \frac{\partial^2 \Psi}{\partial x^2} + \frac{2a\beta h^2}{\pi^2} \frac{\partial^2 \Theta}{\partial x^2} = 0 \tag{15}$$

Multiplying Eqs. (11)- (13) by z and integrating them with respect to z from $-h/2$ to $h/2$, we get

$$\alpha \left(\frac{\partial^2 \Phi}{\partial x^2} - \frac{\pi^2 \Phi}{h^2} \right) + b_1 \left(\frac{\partial^2 \Psi}{\partial x^2} - \frac{\pi^2 \Psi}{h^2} \right) + \frac{b \pi^2 h}{24} \frac{\partial^2 w}{\partial x^2} - \alpha_1 \Phi - \alpha_3 \Psi + \gamma_1 \Theta = \kappa_1 \frac{\partial^2 \Phi}{\partial t^2} \quad (16)$$

$$b_1 \left(\frac{\partial^2 \Phi}{\partial x^2} - \frac{\pi^2 \Phi}{h^2} \right) + \gamma \left(\frac{\partial^2 \Psi}{\partial x^2} - \frac{\pi^2 \Psi}{h^2} \right) + \frac{d \pi^2 h}{24} \frac{\partial^2 w}{\partial x^2} - \alpha_3 \Phi - \alpha_2 \Psi + \gamma_2 \Theta = \kappa_2 \frac{\partial^2 \Psi}{\partial t^2} \quad (17)$$

$$K^* \left(\frac{\partial^2 \Theta}{\partial x^2} - \frac{\pi^2 \Theta}{h^2} \right) = \left(1 + \tau_0 \frac{\partial}{\partial t} \right) \left[-\frac{\beta T_0 \pi^2 h}{24} \frac{\partial}{\partial t} \left(\frac{\partial^2 w}{\partial x^2} \right) + \gamma_1 T_0 \frac{\partial \Phi}{\partial t} + \gamma_2 T_0 \frac{\partial \Psi}{\partial t} + \rho C^* \frac{\partial \Theta}{\partial t} \right] \quad (18)$$

Introducing non-dimensional variables as:

$$x' = \frac{1}{L} x, \quad u' = \frac{1}{L} u, \quad w' = \frac{1}{L} w, \quad t'_x = \frac{t_x}{E}, \quad \Phi' = \frac{L}{\alpha} \Phi, \quad \Theta' = \frac{\beta}{E} \Theta, \quad t' = \frac{c_1}{L} t, \quad \tau'_0 = \frac{c_1}{L} \tau_0, \quad \Psi' = \frac{L}{\alpha} \Psi, \quad (19)$$

where $c_1^2 = \frac{\lambda + 2\mu}{\rho}$ and $E = \frac{\mu(3\lambda + 2\mu)}{\lambda + \mu}$ is Young's Modulus.

Making use of Eq. (19) in Eqs. (15)- (18), we obtain

$$\frac{\partial^4 w}{\partial x^4} + a_1 \left(\frac{\partial^2 w}{\partial t^2} \right) - a_2 \frac{\partial^2 \Phi}{\partial x^2} - a_3 \frac{\partial^2 \Psi}{\partial x^2} + a_4 \frac{\partial^2 \Theta}{\partial x^2} = 0 \quad (20)$$

$$a_5 \frac{\partial^2 \Phi}{\partial x^2} - a_6 \Phi + a_7 \frac{\partial^2 \Psi}{\partial x^2} - a_8 \Psi + a_9 \frac{\partial^2 w}{\partial x^2} - a_{10} \Phi - a_{11} \Psi + a_{12} \Theta - \frac{\partial^2 \Phi}{\partial t^2} = 0 \quad (21)$$

$$a_{13} \frac{\partial^2 \Phi}{\partial x^2} - a_{14} \Phi + a_{15} \frac{\partial^2 \Psi}{\partial x^2} - a_{16} \Psi + a_{17} \frac{\partial^2 w}{\partial x^2} - a_{18} \Phi - a_{19} \Psi + a_{20} \Theta - \frac{\partial^2 \Psi}{\partial t^2} = 0 \quad (22)$$

$$\frac{\partial^2 \Theta}{\partial x^2} - a_{21} \Theta = \left(1 + \tau_0 \frac{\partial}{\partial t} \right) \left[a_{22} \frac{\partial}{\partial t} \left(\frac{\partial^2 w}{\partial x^2} \right) + a_{23} \frac{\partial \Phi}{\partial t} + a_{24} \frac{\partial \Psi}{\partial t} + a_{25} \frac{\partial \Theta}{\partial t} \right] \quad (23)$$

where

$$\begin{aligned} a_1 &= \frac{\rho a h c_1^2 L^2}{I(\lambda + 2\mu)}, a_2 = \frac{2ab\alpha h^2}{I\pi^2(\lambda + 2\mu)}, a_3 = \frac{2ad\alpha h^2}{I\pi^2(\lambda + 2\mu)}, a_4 = \frac{2ah^2 EL}{I\pi^2(\lambda + 2\mu)}, a_5 = \frac{\alpha}{k_1 c_1^2}, a_6 = \frac{\alpha \pi^2 L^2}{k_1 c_1^2 h^2}, \\ a_7 &= \frac{b_1}{k_1 c_1^2}, a_8 = \frac{b_1 \pi^2 L^2}{k_1 c_1^2 h^2}, a_9 = \frac{bh\pi^2 L^2}{24\alpha k_1 c_1^2}, a_{10} = \frac{\alpha_1 L^2}{k_1 c_1^2}, a_{11} = \frac{\alpha_3 L^2}{k_1 c_1^2}, a_{12} = \frac{\gamma_1 EL^3}{\alpha \beta k_1 c_1^2}, a_{13} = \frac{b_1}{k_2 c_1^2}, \\ a_{14} &= \frac{b_1 \pi^2 L^2}{k_2 c_1^2 h^2}, a_{15} = \frac{\gamma}{k_2 c_1^2}, a_{16} = \frac{\gamma \pi^2 L^2}{k_2 c_1^2 h^2}, a_{17} = \frac{dh\pi^2 L^2}{24\alpha k_2 c_1^2}, a_{18} = \frac{\alpha_3 L^2}{k_2 c_1^2}, a_{19} = \frac{\alpha_2 L^2}{k_2 c_1^2}, \\ a_{20} &= \frac{\gamma_2 EL^3}{\alpha \beta k_2 c_1^2}, a_{21} = \frac{\pi^2 L^2}{h^2}, a_{22} = -\frac{T_0 h c_1 \pi^2 \beta^2}{24EK^*}, a_{23} = \frac{\alpha \beta T_0 \gamma_1 c_1}{EK^*}, a_{24} = \frac{\alpha \beta T_0 \gamma_2 c_1}{EK^*}, a_{25} = \frac{\rho C^* c_1 L}{K^*} \end{aligned} \quad (24)$$

5 INITIAL AND BOUNDARY CONDITIONS

The initial conditions of the problem are assumed to be homogeneous and are taken as:

$$\begin{aligned} w(x,t)|_{t=0} = \frac{\partial w(x,t)}{\partial t} \Big|_{t=0} = 0 \quad \Phi(x,t)|_{t=0} = \frac{\partial \Phi(x,t)}{\partial t} \Big|_{t=0} = 0 \\ \Psi(x,t)|_{t=0} = \frac{\partial \Psi(x,t)}{\partial t} \Big|_{t=0} = 0 \quad \Theta(x,t)|_{t=0} = \frac{\partial \Theta(x,t)}{\partial t} \Big|_{t=0} = 0 \end{aligned} \quad (25)$$

These initial conditions are supplemented by considering that the two ends of the micro beam are clamped:

$$w(x,t)|_{x=0,L} = \frac{\partial w(x,t)}{\partial x} \Big|_{x=0,L} = 0 \quad (26)$$

We also assume that the volume fraction fields and the temperature should satisfy the following relation:

$$\Phi(x,t)|_{x=0,L} = 0, \quad \Psi(x,t)|_{x=0,L} = 0, \quad \Theta(x,t)|_{x=0} = \Theta_0 H(t), \quad \Theta(x,t)|_{x=L} = 0. \quad (27)$$

6 SOLUTION IN THE LAPLACE TRANSFORM DOMAIN

Applying the Laplace transform defined by

$$\bar{f}(s) = L[f(t)] = \int_0^{\infty} f(t) e^{-st} dt \quad (28)$$

On the Eqs. (20)- (23) under the initial conditions (25), after some simplifications, we obtain

$$\left(\frac{d^{10}}{dx^{10}} + B_1 \frac{d^8}{dx^8} + B_2 \frac{d^6}{dx^6} + B_3 \frac{d^4}{dx^4} + B_4 \frac{d^2}{dx^2} + B_5 \right) (\bar{w}, \bar{\Phi}, \bar{\Psi}, \bar{\Theta}) = 0 \quad (29)$$

B_1, B_2, B_3, B_4, B_5 , are given in the Appendix A.

The solution of the Eqs.(31), in the Laplace transform domain can be written as:

$$(\bar{w}, \bar{\Phi}, \bar{\Psi}, \bar{\Theta}) = \sum_{i=1}^5 (1, g_{1i}, g_{2i}, g_{3i}) \{ D_i e^{-\lambda_i x} + D_{i+5} e^{\lambda_i x} \} \quad (30)$$

$g_{1i}, g_{2i}, g_{3i}; (i = 1, 2, 3, 4, 5)$ are given in the Appendix B.

Here $\pm \lambda_i$, $i = 1, 2, 3, 4, 5$ are the roots of the characteristic equation

$$\lambda^{10} + B_1 \lambda^8 + B_2 \lambda^6 + B_3 \lambda^4 + B_4 \lambda^2 + B_5 = 0 \quad (31)$$

On using Eqs. (31) in Eqs. (5) and with the help of Eqs. (14) and (19), we obtain the corresponding expressions for axial displacement and axial stress in the Laplace transform domain as:

$$\bar{u} = -z \sum_{i=1}^5 \left(-\lambda_i D_i e^{-\lambda_i x} + \lambda_i D_{i+5} e^{\lambda_i x} \right) \tag{32}$$

$$\bar{t}_x = \sum_{i=1}^5 \left[P_1 z \lambda_i^2 + \sin(\pi z / h) \{ P_2 g_{1i} + P_3 g_{2i} - g_{3i} \} \right] \left(D_i e^{-\lambda_i x} + D_{i+5} e^{\lambda_i x} \right) \tag{33}$$

The boundary conditions (26), (27) in the Laplace transform domain take the form as:

$$\bar{w}(x, s) \Big|_{x=0,L} = \frac{d\bar{w}(x, s)}{dx} \Big|_{x=0,L} = 0, \quad \bar{\Phi}(x, s) \Big|_{x=0,L} = 0, \quad \bar{\Psi}(x, s) \Big|_{x=0,L} = 0, \quad \bar{\Theta}(x, s) \Big|_{x=0} = \frac{\Theta_0}{s} = \bar{F}(s), \quad \bar{\Theta}(x, s) \Big|_{x=L} = 0. \tag{34}$$

In order to determine the unknowns parameters, substituting Eqs.(30) in the boundary conditions (34), we obtain a system of ten linear equations in the matrix form as:

$$\begin{bmatrix} D_1 \\ D_2 \\ D_3 \\ D_4 \\ D_5 \\ D_6 \\ D_7 \\ D_8 \\ D_9 \\ D_{10} \end{bmatrix} = \begin{bmatrix} 1 & 1 & 1 & 1 & 1 & 1 & 1 & 1 & 1 & 1 \\ e^{-\lambda_1 L} & e^{-\lambda_2 L} & e^{-\lambda_3 L} & e^{-\lambda_4 L} & e^{-\lambda_5 L} & e^{\lambda_1 L} & e^{\lambda_2 L} & e^{\lambda_3 L} & e^{\lambda_4 L} & e^{\lambda_5 L} \\ -\lambda_1 & -\lambda_2 & -\lambda_3 & -\lambda_4 & -\lambda_5 & \lambda_1 & \lambda_2 & \lambda_3 & \lambda_4 & \lambda_5 \\ -\lambda_1 e^{-\lambda_1 L} & -\lambda_2 e^{-\lambda_2 L} & -\lambda_3 e^{-\lambda_3 L} & -\lambda_4 e^{-\lambda_4 L} & -\lambda_5 e^{-\lambda_5 L} & \lambda_1 e^{\lambda_1 L} & \lambda_2 e^{\lambda_2 L} & \lambda_3 e^{\lambda_3 L} & \lambda_4 e^{\lambda_4 L} & \lambda_5 e^{\lambda_5 L} \\ g_{11} & g_{12} & g_{13} & g_{14} & g_{15} & g_{11} & g_{12} & g_{13} & g_{14} & g_{15} \\ g_{11} e^{-\lambda_1 L} & g_{12} e^{-\lambda_2 L} & g_{13} e^{-\lambda_3 L} & g_{14} e^{-\lambda_4 L} & g_{15} e^{-\lambda_5 L} & g_{11} e^{\lambda_1 L} & g_{12} e^{\lambda_2 L} & g_{13} e^{\lambda_3 L} & g_{14} e^{\lambda_4 L} & g_{15} e^{\lambda_5 L} \\ g_{21} & g_{22} & g_{23} & g_{24} & g_{25} & g_{21} & g_{22} & g_{23} & g_{24} & g_{25} \\ g_{21} e^{-\lambda_1 L} & g_{22} e^{-\lambda_2 L} & g_{23} e^{-\lambda_3 L} & g_{24} e^{-\lambda_4 L} & g_{25} e^{-\lambda_5 L} & g_{21} e^{\lambda_1 L} & g_{22} e^{\lambda_2 L} & g_{23} e^{\lambda_3 L} & g_{24} e^{\lambda_4 L} & g_{25} e^{\lambda_5 L} \\ g_{31} & g_{32} & g_{33} & g_{34} & g_{35} & g_{31} & g_{32} & g_{33} & g_{34} & g_{35} \\ g_{31} e^{-\lambda_1 L} & g_{32} e^{-\lambda_2 L} & g_{33} e^{-\lambda_3 L} & g_{34} e^{-\lambda_4 L} & g_{35} e^{-\lambda_5 L} & g_{31} e^{\lambda_1 L} & g_{32} e^{\lambda_2 L} & g_{33} e^{\lambda_3 L} & g_{34} e^{\lambda_4 L} & g_{35} e^{\lambda_5 L} \end{bmatrix}^{-1} \begin{bmatrix} 0 \\ 0 \\ 0 \\ 0 \\ 0 \\ 0 \\ 0 \\ 0 \\ \bar{F}(s) \\ 0 \end{bmatrix} \tag{35}$$

On solving the above system of Eqs. (35), we obtain the values of unknown parameters $D_i, i = 1, 2, \dots, 10$. This completes the solution of the problem in Laplace transform domain.

7 PARTICULAR CASES

If $\tau_0 = 0$, in Eqs. (30) along with Eqs. (35) yield the corresponding expressions for a thermoelastic double porous micro beam in the context of coupled theory (CT) of thermoelasticity. These results are same if we solve the problem directly.

If $b_1 = \alpha_3 = \gamma = \alpha_2 = \gamma_2 = d \rightarrow 0$ in Eqs. (30) along with Eqs.(35), we obtain the corresponding expressions for a thermoelastic micro beam with single porosity (thermoelastic micro beam with voids) which is same as investigated by Sharma and Grover [28].

8 INVERSION OF THE LAPLACE DOMAIN

To determine the displacement, stresses and temperature distribution in the physical domain, we will adopt a numerical inversion method given by [37]. In this method, Laplace domain $\bar{f}(s)$ can be inverted to time domain $f(t)$ as:

$$f(t) = \frac{e^{\Omega t}}{t_1} \left[\frac{1}{2} \bar{f}(\Omega) + \operatorname{Re} \sum_{k=1}^N \bar{f} \left(\Omega + \frac{ik\pi}{t_1} \right) \exp \left(\frac{ik\pi t}{t_1} \right) \right], \quad 0 < t_1 < 2t$$

where Re is the real part and i is the imaginary number unit. The value of N is chosen sufficiently large and it represents the number of terms in the truncated Fourier series such that

$$f(t) = \exp(\Omega t) \operatorname{Re} \left[\bar{f} \left(\Omega + \frac{iN\pi}{t_1} \right) \exp \left(\frac{iN\pi t}{t_1} \right) \right] \leq \varepsilon_1$$

ε_1 is a prescribed small positive number. Also, the value of Ω should satisfy the relation $\Omega t \approx 4.7$ for the faster convergence [38].

9 NUMERICAL RESULTS AND DISCUSSION

Numerical computations have been done for thermoelastic material with double porosity structure with the following mechanical and thermal properties. The material parameters are taken as in [39, 40]

$$\begin{aligned} \lambda &= 2.17 \times 10^{10} \text{ Nm}^{-2}, C^* = 1.04 \times 10^3 \text{ m}^2 \text{ s}^{-2} \text{ K}^{-1}, \mu = 1.639 \times 10^{10} \text{ Nm}^{-2}, K^* = 1.7 \times 10^2 \text{ N s}^{-1} \text{ K}^{-1}, \\ T_0 &= 298 \text{ K}, \rho = 1.74 \times 10^3 \text{ Kgm}^{-3}, \alpha_1 = 3.688 \times 10^{-5} \text{ K}^{-1}, \tau_0 = 0.09 \times 10^{-10} \text{ s}, \alpha = 1.3 \times 10^{-5} \text{ N}, \\ \alpha_2 &= 2.4 \times 10^{10} \text{ Nm}^{-2}, \alpha_3 = 2.5 \times 10^{10} \text{ Nm}^{-2}, \gamma = 1.1 \times 10^{-5} \text{ N}, \gamma_1 = 0.16 \times 10^5 \text{ Nm}^{-2}, b_1 = 0.12 \times 10^{-5} \text{ N} \\ d &= 0.1 \times 10^{10} \text{ Nm}^{-2}, \gamma_2 = 0.219 \times 10^5 \text{ Nm}^{-2}, \kappa_1 = 0.1456 \times 10^{-12} \text{ Nm}^{-2} \text{ s}^2, b = 0.9 \times 10^{10} \text{ Nm}^{-2} \\ \alpha_1 &= 2.3 \times 10^{10} \text{ Nm}^{-2}, \kappa_2 = 0.1546 \times 10^{-12} \text{ Nm}^{-2} \text{ s}^2 \end{aligned}$$

The aspect ratio of the beam is fixed as $L/h = 10$, $a/h = 0.5$, $x_3 = h/6$. The software MATLAB has been used to find the values of lateral deflection, axial stress, axial displacement, volume fraction field and temperature distribution. The variations of these quantities with respect to axial distance have been shown in Figs. 2- 6 to show the effect of porosity. In Figs. 2- 6, solid line corresponds to thermoelastic double porous micro beam (TDP) and small dashes line corresponds to thermoelastic single porous micro beam (TSP). Also, the effect of thermal relaxation time is depicted graphically in Figs.7-11. In Figs. 7- 11, solid line corresponds to Lord-Shulman (LS) theory of thermoelasticity and small dashes line corresponds to coupled (CT) theory of thermoelasticity.

9.1 Effect of porosity

Fig.2 shows the variation of lateral deflection w with respect to axial distance x . It is found that for TDP, the value of lateral deflection w initially increases for the region $1 < x \leq 2.0$, decreases for $2.0 < x \leq 3.0$ and then increases afterwards as $x > 3.0$. In case of TSP, value of w initially decreases for the region $1 < x \leq 2.0$, increases for $2.0 < x \leq 3.8$ and becomes almost stationary for the remaining region. Due to effect of porosity, the magnitude values remain more for TSP in comparison to that of TDP for all the values of x . Fig.3 depicts the variation of axial stress t_x with respect to axial distance x . It is evident that the value of axial stress t_x initially decreases for $1 \leq x \leq 2$ and then increases for the remaining region as $x > 2$ for both TDP and TSP. The trend and behavior of variation is similar for both TDP and TSP with difference in the magnitude values only. The values are higher for TSP than that of TDP for all the values of x due to the effect of porosity.

Fig. 4 shows the variation of volume fraction field ϕ with respect to axial distance x . It is clear from figure that for TDP, the value of volume fraction field ϕ decreases initially and then increases slowly and steadily as $x > 2$ whereas in case of TSP, ϕ increases for the region $1 \leq x \leq 2$, decreases for $2 < x \leq 3$ and then become almost

stationary as $x > 3$. It is also found that due to porosity effect, the value of φ remain more for TSP as compared to that of the values of TDP.

Fig.5 represents the variation of temperature distribution T with respect to axial distance x . It is noticed that for TDP, the value of temperature distribution T initially decreases for $1 \leq x \leq 2$ and then increases monotonically with increase in the value of x whereas for TSP, it increases for the region $1 \leq x \leq 2$ and then start decreasing as $x > 2$. The trend and behavior of variation is opposite to each other for all the values of x and the magnitude values of T are higher in case of TDP than that of the values of TSP due to the effect of porosity. Fig.6 depicts the variation of axial displacement u with respect to axial distance x . It is found that the value of axial displacement u increases for the region $1 \leq x \leq 2$, decreases for $2 < x \leq 3$ and then become almost stationary in the subsequent region for both TDP and TSP. Although, similar type of pattern of variation is shown by both TDP and TSP, but the magnitude values are more for TSP in comparison to TDP due to the effect of porosity.

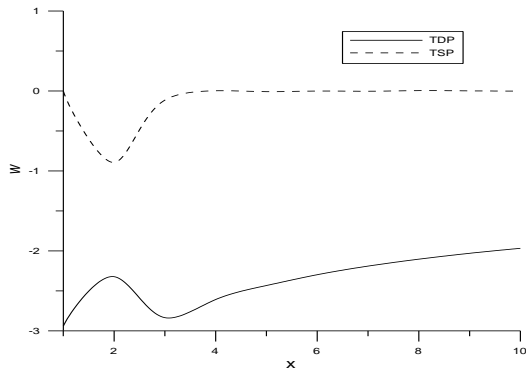


Fig.2
Variation of lateral deflection w w.r.t. axial distance x .

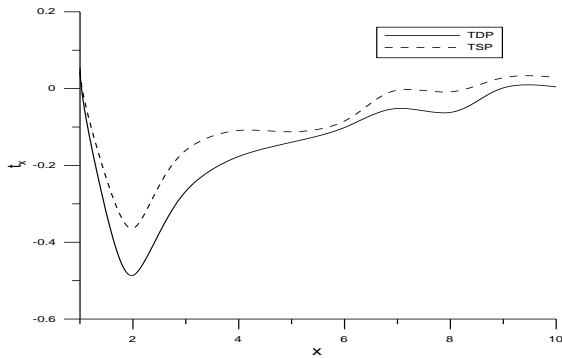


Fig.3
Variation of axial stress t_x w.r.t. axial distance x .

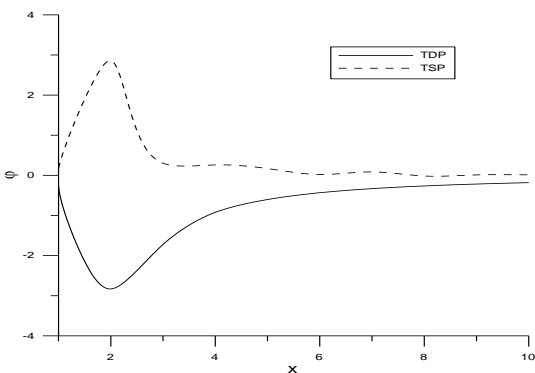


Fig.4
Variation of volume fraction field φ w.r.t. axial distance x .

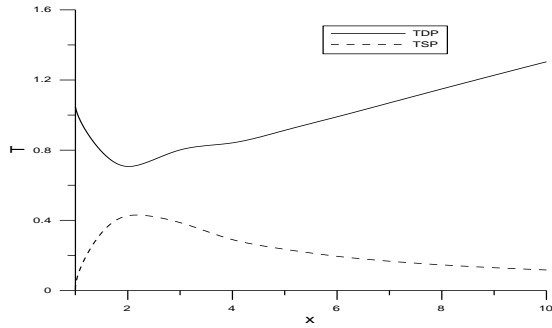


Fig.5
Variation of temperature distribution T w.r.t. axial distance x .

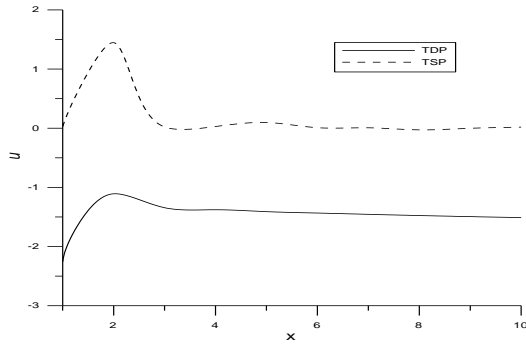


Fig.6
Variation of axial displacement u w.r.t. axial distance x .

9.2 Effect of thermal relaxation time

Fig.7 depicts that the value of lateral deflection w increases for the region $1 < x \leq 2$, decreases for $2 < x \leq 3$ and increases afterwards with the increase in the value of axial distance x . Due to effect of relaxation time parameter, the values of w are more for CT theory of thermoelasticity in comparison to the values for LS theory of thermoelasticity. Fig.8, it is noticed that the value of axial stress t_x initially decreases for $1 < x \leq 2$ and then increases in the remaining region as $x > 2$. The trend and behavior of variation is similar for LS and CT theories of thermoelasticity but the magnitude values are higher in case of LS theory due to effect of relaxation time parameter. Fig.9 shows that the values of volume fraction field ϕ initially decreases and then increases slowly and steadily as $x > 2$. It is also found that relaxation time effect decreases the magnitude values of ϕ for LS theory as compared to CT theory of thermoelasticity. Fig.10 represents that the value of temperature distribution T initially decreases for the region $1 < x \leq 2$ and then increases monotonically with increase in the value of x . The trend of variation is of similar type but the magnitude values are more for LS theory than that of CT theory of thermoelasticity due to the effect of relaxation time. Fig.11, it is evident that value of axial displacement u increases for the region $1 < x \leq 2$ and then decreases afterwards in the remaining region. Although, the trend and behavior of variation remains the same with the difference in magnitude values only. The relaxation time parameter decreases the magnitude values of u for LS theory as compared to CT theory of thermoelasticity.

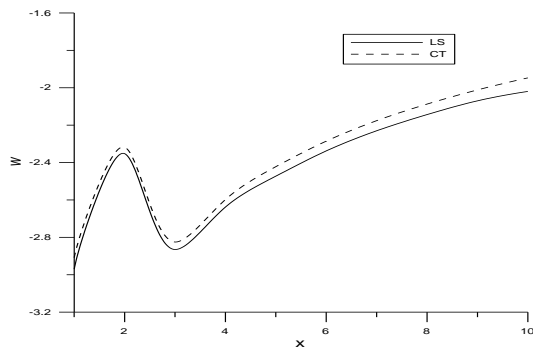


Fig.7
Variation of lateral deflection w w.r.t. axial distance x .

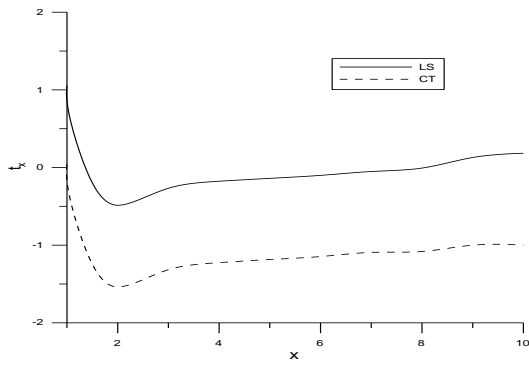


Fig.8
Variation of axial stress t_x w.r.t. axial distance x .

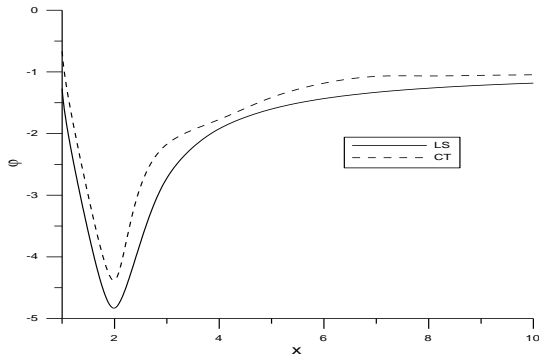


Fig.9
Variation of volume fraction field φ w.r.t. axial distance x .

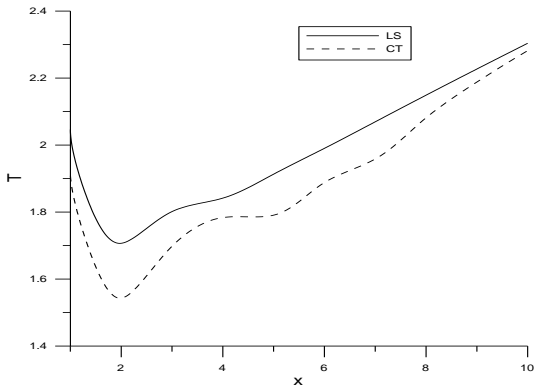


Fig.10
Variation of temperature distribution T w.r.t. axial distance x .

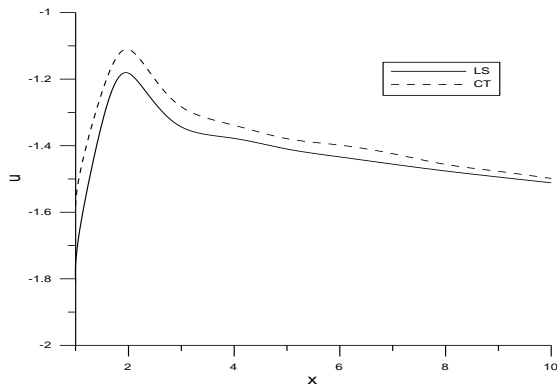


Fig.11
Variation of axial displacement u w.r.t. axial distance x .

10 CONCLUSIONS

In the present work, vibration analysis of a thermoelastic double porous micro beam based on the Euler-Bernoulli theory, in the context of Lord-Shulman theory of thermoelasticity has been studied. Variations of axial displacement, axial stress, lateral deflection, volume fraction field and temperature distribution with axial distance are depicted graphically to show the effects of porosity and thermal relaxation time. It is found that porosity has a significant effect on the all the physical quantities. It has both increasing as well as decreasing effect on the resulting quantities. It is observed that due to effect of porosity, the values of axial displacement, axial stress, lateral deflection and volume fraction field are more for thermoelastic micro beam with single porosity in comparison to the values for thermoelastic micro beam with double porosity whereas an opposite trend and behavior of variation is noticed in case of temperature distribution. Also, all the field quantities are observed to be very sensitive towards the thermal relaxation time parameter. The thermal relaxation time parameter decreases the magnitude values of axial displacement, lateral deflection and volume fraction field for LS theory in comparison to CT theory of thermoelasticity whereas trend gets reversed in case of axial stress and temperature distribution which shows that it is very important to take into account the thermal relaxation time parameter.

This type of study is useful due to its physical application in geophysics, rock mechanics, mechanical engineering, civil engineering and industrial sectors. The results obtained in this investigation should prove to be beneficial for the researchers working on the theory of thermoelasticity with double porosity structure. The introduction of double porous parameter to the thermoelastic medium represents a more realistic model for further studies.

APPENDIX A

$$\begin{aligned}
 a_{26} &= s(1 + \tau_0 s), a_{27} = -s(1 + \tau_0 s)a_{22}, a_{28} = -s(1 + \tau_0 s)a_{23}, a_{29} = -s(1 + \tau_0 s)a_{24}, a_{30} = -\{a_{21} + s(1 + \tau_0 s)a_{25}\}, \\
 n_1 &= -(a_6 + a_{10} + s^2), n_2 = -(a_8 + a_{11}), n_3 = -(a_{18} + a_{14}), n_4 = -(a_{16} + a_{19} + s^2), \\
 r_1 &= a_5 a_{15} - a_7 a_{13}, r_2 = a_5(a_{15} a_{30} + n_4) - a_{13} n_2 + n_1 a_{15} - a_7(a_{13} a_{30} + n_3), \\
 r_3 &= n_1(a_{15} a_{30} + n_4) + a_5(n_4 a_{30} - a_{20} a_{29}) - a_7(n_3 a_{30} - a_{20} a_{28}) - n_2(a_{13} a_{30} + n_3) + a_{12}(a_{13} a_{29} - a_{15} a_{28}), \\
 r_4 &= n_1(n_4 a_{30} - a_{20} a_{29}) + a_{12}(n_3 a_{29} - n_4 a_{28}) + n_2(a_{20} a_{28} - n_3 a_{30}), r_5 = a_9 a_{15} - a_7 a_{17}, \\
 r_6 &= a_9(a_{15} a_{30} + n_4) - a_7(a_{17} a_{30} - a_{20} a_{27}) - n_2 a_{17} - a_{12} a_{15} a_{27}, \\
 r_7 &= a_9(n_4 a_{30} - a_{20} a_{29}) + a_{12}(a_{17} a_{29} - n_4 a_{27}) - n_2(a_{17} a_{30} - a_{20} a_{27}), \\
 r_8 &= a_9 a_{13} - a_5 a_{17}, r_9 = a_9(a_{13} a_{30} + n_3) - n_1 a_{17} - a_5(a_{17} a_{30} - a_{20} a_{27}) - a_{12} a_{10} a_{27}, \\
 r_{10} &= a_9(n_3 a_{30} - a_{20} a_{28}) - n_1(a_{30} a_{17} - a_{27} a_{20}) + a_{12}(a_{17} a_{28} - n_3 a_{27}), \\
 r_{11} &= a_{27}(a_5 a_{12} + a_7 a_{13}), r_{12} = a_9(a_{13} a_{29} - a_{15} a_{28}) + a_5(n_4 a_{27} - a_{17} a_{29}) + a_{27}(n_1 a_{15} + g_3 a_{13}) \\
 &\quad - a_7(a_{17} a_{28} - n_3 a_{27}), r_{13} = a_9(n_3 a_{29} - n_4 a_{28}) - n_1(a_{17} a_{29} - n_4 a_{27}) - n_2(a_{17} a_{28} - n_3 a_{27}), \\
 B_1 &= (r_2 + a_2 r_5 - a_3 r_8 - a_4 r_{11})/r_1, B_2 = (a_1 r_1 s^2 + a_2 r_6 - a_3 r_9 - a_4 r_{12} + r_3)/r_1, \\
 B_3 &= (a_1 r_3 s^2 + a_2 r_7 - a_3 r_{10} - a_4 r_{13} + r_4)/r_1, B_4 = (a_1 r_3 s^2)/r_1, B_5 = (a_1 r_4 s^2)/r_1 \\
 P_1 &= -\frac{(\lambda + 2\mu)}{E}, P_2 = \frac{b\alpha}{EL}, P_3 = \frac{d\alpha}{EL}
 \end{aligned}$$

APPENDIX B

$$\begin{aligned}
 g_{1i} &= -\{r_5 \lambda_i^6 + r_6 \lambda_i^4 + r_7 \lambda_i^2\} / \{r_1 \lambda_i^6 + r_2 \lambda_i^4 + r_3 \lambda_i^2 + r_4\}, \quad g_{2i} = \{r_8 \lambda_i^6 + r_9 \lambda_i^4 + r_{10} \lambda_i^2\} / \{r_1 \lambda_i^6 + r_2 \lambda_i^4 + r_3 \lambda_i^2 + r_4\}, \\
 g_{3i} &= -\{r_{11} \lambda_i^6 + r_{12} \lambda_i^4 + r_{13} \lambda_i^2\} / \{r_1 \lambda_i^6 + r_2 \lambda_i^4 + r_3 \lambda_i^2 + r_4\}; \quad i = 1, 2, 3, \dots, 5
 \end{aligned}$$

REFERENCES

- [1] Lord H., Shulman Y., 1967, A generalized dynamical theory of thermoelasticity, *Journal of the Mechanics and Physics of Solids* **15**: 299-309.
- [2] Biot M. A., 1941, General theory of three-dimensional consolidation, *Journal of Applied Physics* **12**: 155-164.
- [3] Barenblatt G. I., Zheltov I. P., Kochina I. N., 1960, Basic concept in the theory of seepage of homogeneous liquids in fissured rocks (strata), *Journal of Applied Mathematics and Mechanics* **24**: 1286-1303.
- [4] Aifantis E. C., 1977, Introducing a multi-porous medium, *Developments in Mechanics* **8**: 209-211.
- [5] Aifantis E. C., 1979, On the response of fissured rocks, *Developments in Mechanics* **10**: 249-253.
- [6] Aifantis E. C., 1980, On the problem of diffusion in solids, *Acta Mechanica* **37**: 265-296.
- [7] Wilson R.K., Aifantis E.C., 1984, On the theory of consolidation with double porosity, *International Journal of Engineering Science* **20**(9):1009-1035.
- [8] Khaled M. Y., Beskos D. E., Aifantis E.C., 1984, On the theory of consolidation with double porosity-III, *International Journal for Numerical and Analytical Methods in Geomechanics* **8**: 101-123.
- [9] Beskos D.E., Aifantis E.C., 1986, On the theory of consolidation with double porosity-II, *International Journal of Engineering Science* **24**: 1697-1716.
- [10] Khalili N., Salvadorian A. P. S., 2003, A fully coupled constitutive model for thermo-hydro-mechanical analysis in elastic media with double porosity, *Geophysical Research Letters* **30**: 2268-2271.
- [11] Svanadze M., 2005, Fundamental solution in the theory of consolidation with double porosity, *Journal of the Mechanical Behavior of Materials* **16**: 123-130.
- [12] Svanadze M., 2012, Plane waves and boundary value problems in the theory of elasticity for solids with double porosity, *Acta Applicandae Mathematicae* **122**: 461-470.
- [13] Straughan B., 2013, Stability and uniqueness in double porosity elasticity, *International Journal of Engineering Science* **65**: 1-8.
- [14] Nunziato J.W., Cowin S.C., 1979, A nonlinear theory of elastic materials with voids, *Archive for Rational Mechanics and Analysis* **72**: 175-201.
- [15] Cowin S.C., Nunziato J.W., 1983, Linear elastic materials with voids, *Journal of Elasticity* **13**: 125-147.
- [16] Iesan D., Quintanilla R., 2014, On a theory of thermoelastic materials with a double porosity structure, *Journal of Thermal Stresses* **37**: 1017-1036.
- [17] Fritz J., Baller M.K., Lang H.P., Rothuizen H., Vettiger P., Meyer E., Gntherodt H.J., Gerber C., Gimzewski J.K., 2001, Translating bio-molecular recognition into nanomechanics, *Science* **288**: 316-318.
- [18] Sidles J. A., 1991, Noninductive detection of single proton-magnetic resonance, *Applied Physics Letters* **58**: 2854-2856.
- [19] Nabian A., Rezazadeh G., Haddad-derafshi M., Tahmasebi A., 2008, Mechanical behavior of a circular micro plate subjected to uniform hydrostatic and non-uniform electrostatic pressure, *Microsystem Technologies* **14**: 235-240.
- [20] Fathalilou M., Motallebi A., Rezazadeh G., Yagubizade H., Shirazi K., Alizadeh Y., 2009, Mechanical behavior of an electrostatically-actuated microbeam under mechanical shock, *Journal of Solid Mechanics* **1**: 45-57.
- [21] Dimarogonas A., 1996, *Vibration for Engineers*, Prentice-Hall, Inc.
- [22] Meirovitch L., 2001, *Fundamentals of Vibrations*, McGraw-Hill, International Edition.
- [23] Boley B.A., 1972, Approximate analyses of thermally induced vibrations of beams and plates, *Journal of Applied Mechanics* **39**: 212-216.
- [24] Manolis G.D., Beskos D.E., 1980, Thermally induced vibrations of beam structures, *Computer Methods in Applied Mechanics and Engineering* **21**: 337-355.
- [25] Al-Hunithi N.S., Al-Nimir M.A., Najj M., 2001, Dynamic response of a rod due to a moving heat source under the hyperbolic heat conduction model, *Journal of Sound and Vibration* **242**: 629-640.
- [26] Biondi B., Caddemi S., 2005, Closed form solutions of Euler-Bernoulli beams with singularities, *International Journal of Solids and Structures* **42**: 3027-3044.
- [27] Fang D.N., Sun Y.X., Soh A.K., 2006, Analysis of frequency spectrum of laser-induced vibration of micro beam resonators, *Chinese Physics Letters* **23**: 1554-1557.
- [28] Sharma J.N., Grover D., 2011, Thermoelastic vibrations in micro-/nano-scale beam resonators with voids, *Journal of Sound and Vibration* **330**: 2964-2977.
- [29] Esen I., 2015, A new FEM procedure for transverse and longitudinal vibration analysis of thin rectangular plates subjected to a variable velocity moving load along an arbitrary trajectory, *Latin American Journal of Solids and Structures* **12**: 808-830.
- [30] Kumar R., 2016, Response of thermoelastic beam due to thermal source in modified couple stress theory, *Computational Methods in Science and Technology* **22**(2): 95-101.
- [31] Ghadiri M., Shafiei N., 2016, Vibration analysis of rotating functionally graded Timoshenko micro beam based on modified couple stress theory under different temperature distributions, *Acta Astronautica* **121**: 221-240.
- [32] Zenkour A. M., 2016, Free vibration of a microbeam resting on Pasternak's foundation via the GN thermoelasticity theory without energy dissipation, *Journal of Low Frequency Noise, Vibration and Active Control* **35**(4): 303-311.

- [33] Kaghazian A., Hajnayeb A., Foruzande H., 2017, Free vibration analysis of a piezoelectric nanobeam using nonlocal elasticity theory, *Structural Engineering and Mechanics* **61**(5): 617-624.
- [34] Ebrahimi F., Barati M.R., 2017, Vibration analysis of embedded size dependent FG nanobeams based on third-order shear deformation beam theory, *Structural Engineering and Mechanics* **61**(6): 721-736.
- [35] Zenkour A. M., 2017, Thermoelastic response of a micro beam embedded in Visco-Pasternak's medium based on GN-III model, *Journal of Thermal Stresses* **40**(2): 198-210.
- [36] Arefi M., Zenkour A.M., 2017, Vibration and bending analysis of a sandwich micro beam with two integrated piezomagnetic face-sheet, *Composite Structures* **159**: 479-490.
- [37] Honig G., Hirdes U., 1984, A method for the numerical inversion of the Laplace transforms, *Journal of Computational and Applied Mathematics* **10**: 113-132.
- [38] Tzou D., 1996, *Macro-to-Micro Heat transfer*, Taylor& Francis, Washington DC.
- [39] Sherief H., Saleh H., 2005, A half space problem in the theory of generalized thermoelastic diffusion, *International Journal of Solids and Structures* **42**: 4484-4493.
- [40] Khalili N., 2003, Coupling effects in double porosity media with deformable matrix, *Geophysical Research Letters* **30**(22): 2153-2155.